Accepted Manuscript

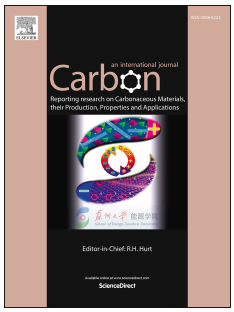

Successful functionalization of superporous zeolite templated carbon using aminobenzene acids and electrochemical methods

Carolina González-Gaitán, Ramiro Ruiz-Rosas, Hirotomo Nishihara, Takashi Kyotani, Emilia Morallón, Diego Cazorla-Amorós

PII: S0008-6223(15)30497-8

DOI: 10.1016/j.carbon.2015.12.006

Reference: CARBON 10551

To appear in: *Carbon*

Received Date: 23 October 2015

Revised Date: 30 November 2015

Accepted Date: 3 December 2015

Please cite this article as: C. González-Gaitán, R. Ruiz-Rosas, H. Nishihara, T. Kyotani, E. Morallón, D. Cazorla-Amorós, Successful functionalization of superporous zeolite templated carbon using aminobenzene acids and electrochemical methods, *Carbon* (2016), doi: 10.1016/j.carbon.2015.12.006.

SUCCESSFUL FUNCTIONALIZATION OF SUPERPOROUS ZEOLITE TEMPLATED CARBON USING AMINOBENZENE ACIDS AND ELECTROCHEMICAL METHODS

Carolina González-Gaitán[a], Ramiro Ruiz-Rosas[a], Hirotomo Nishihara[b], Takashi Kyotani[b], Emilia Morallón[a], Diego Cazorla-Amorós[a*]

[a] Materials Institute of Alicante (IUMA), University of Alicante, Ap. 99, 03080, Alicante, Spain

[b] Institute of Multidisciplinary Research for Advanced Materials (IMRAM), Tohoku University, Sendai 980-8577, Japan

ABSTRACT

A novel and selective electrochemical functionalization of a highly reactive superporous zeolite templated carbon (ZTC) with two different aminobenzene acids (2-aminobenzoic and 4-aminobenzoic acid) was achieved. The functionalization was done through potentiodynamic treatment in acid media under oxidative conditions, which were optimized to preserve the unique ZTC structure. Interestingly, it was possible to avoid the electrochemical oxidation of the highly reactive ZTC structure by controlling the potential limit of the potentiodynamic experiment in presence of aminobenzene acids. The electrochemical characterization demonstrated the formation of polymer chains along with covalently bonded functionalities to the ZTC surface. The functionalized ZTCs showed several redox processes, producing a capacitance increase in both basic and acid media. The rate performance showed that the capacitance increase is retained at scan rates as high as 100 mVs^{-1}, indicating that there is a fast charge transfer between the polymer chains formed inside the ZTC porosity or the new surface functionalities and the ZTC itself. The success of the proposed approach was also confirmed by using other characterization techniques, which confirmed the presence of different nitrogen groups in the ZTC surface. This promising method could be used to achieve highly selective functionalization of highly porous carbon materials.

*Corresponding author. Tel. +34965903946. E-mail: cazorla@ua.es

1. INTRODUCTION

Zeolite template carbons constitute a family of highly porous nanostructured carbon materials which are prepared using a zeolite as hard template. After filling the porosity of the zeolite with carbon, the zeolite is removed, releasing a negative carbon replica of the parent structure. If the synthesis conditions are properly selected, a kind of highly microporous material being composed by a few stacked (or even one) graphene layers of high curvature can be obtained, showing outstanding electrochemical properties [1]. An illustrative example of such materials is the Zeolite Templated Carbon (ZTC) obtained using the zeolite Y as template [2]. ZTC has a well-defined, ordered and highly interconnected microporosity, high specific surface area (reaching values close to 4000 m^2 g^{-1}), large number of edge sites and high ordered structure, similar to the parent zeolite. Because of its properties, this carbon material is very interesting for fundamental studies, and also shows a high potential for different applications, i.e. adsorption, electrode for EDLC, catalyst support, energy storage and fuel cells [1], [3]. Moreover, the controlled modification of the surface chemistry of this extraordinary material could enhance its properties for the applications mentioned above or other fields.

However, due to the high reactivity of ZTC and the high concentration of edge sites, its functionalization avoiding important structural changes is a challenge. As an example, the introduction of surface oxygen groups through conventional chemical oxidation produces a strong damage of the 3D-dimensionally ordered structure [4]. It was found that the use of electrochemical techniques can control the process with high accuracy without high structural changes [4], [5]. This is because electrochemical techniques have several advantages compared to the conventional chemical routes: i) they are simple and can be immediately interrupted, providing a better control on the time of the treatment, ii) can be run at room temperature and atmospheric pressure, iii) can work with small amount of reagents and sample, iv) the reaction conditions are very reproducible and, v) they are processes with very high sensitivity and selectivity [6].

The modification of ZTC with other heteroatoms like N-containing functional groups would open new possibilities for new applications. It is known that the generation of nitrogen surface groups is of high interest due to the number of applications that are available for nitrogen-doped carbon materials. Among others, they are of interest for increasing the electrochemical activity of carbon materials in the oxygen reduction reaction [7], [8]; for increasing the capacitance, rate performance and durability as electrodes of supercapacitors [9]–[11]; for enhancement of gas and liquid adsorption of acid adsorbates [12]; for the preparation of novel heterogeneous catalysts [13], [14] and for the immobilization of bio-molecules [15]. The synthesis of N-containing ZTC is done using chemical vapor deposition during its synthesis with which N-species are incorporated in the carbon network [16]–[20]; however, it is not possible to control the type of N-species and it inevitably becomes diverse. Post-synthesis modification without structure destruction of ZTC would be a highly desirable method for selective introduction of specific N-containing functional groups.

Electrochemical techniques have been successfully used for the covalent and non-covalent functionalization of different carbon materials with nitrogen functional groups [21], [22] and polymers [23], [24]. The modification of carbon nanotubes using 4-aminobenzoic acid (4-ABA), 4-aminobenzenesulfonic acid (4-ABSA) and 4-aminobenzylphosphonic acid (4-ABPA) in aqueous solution, is an illustrative example of the potential of this method to functionalize with different heteroatoms [8], [25]–[27].

Considering the potential improvement for several applications of modified ZTC with different nitrogen functionalities, in this study, we will use electrochemical methods to introduce N-species in the ZTC taking into account that the experimental conditions can be precisely controlled and that different N-containing molecules can be used, thus increasing the possibilities of modification of the chemical properties of the carbon material. We will analyze the electrochemical functionalization of ZTC with two different aminobenzene acids: 2-aminobenzoic acid (2-ABA) and 4-aminobenzoic acid (4-ABA). The acids have the carboxylic group in *ortho*- and *para*-positions in their structure, respectively, and it determines the

reactivity and possible polymerization over the ZTC surface. The study of the electrochemical functionalization includes different conditions that are tested in order to preserve the ZTC structure after introducing new functionalities on its surface, giving possible routes for a controlled modification. The influence of such functionalization on the electrochemical behavior of ZTC is also determined in this work.

2. EXPERIMENTAL

2.1. ZTC synthesis

ZTC was prepared using zeolite Y (Na-form, SiO_2/Al_2O_3 = 5.6, obtained from Tosoh Co. Ltd.) as a template by the method reported elsewhere [4], [5], [28] . 2 and 4-aminobenzoic acids (2-ABA and 4-ABA, respectively), sulfuric acid (1 M), perchloric acid (70%), and the potassium hydroxide were purchased from Wako Chemicals GmbH.

2.2. Electrochemical modification of ZTC

The working electrode was prepared with a paste of ZTC consisting of ZTC, acetylene black (Denka black, Denki Kagaku Kogyo Kabushiki Kaisha) as a conductive promoter and PTFE (Du Pont-Mitsui Fluorochemicals Company, Ltd.) as binder in a proportion 90:5:5, respectively. A squared-molded ZTC dry paste containing ~6 mg of ZTC and 1 cm^2 was placed in a Pt mesh and pressed at 300 kg cm^{-2} for 5 min. The electrode was dried for 6 h in vacuum, in order to remove all the humidity and adsorbed gases from the carbon porosity, and thus allowing accurate determination of the active phase using in the experiments.

The electrochemical modification of ZTC was performed in a three-electrode cell, with the working electrode prepared as mentioned above, a platinum wire as counter electrode and Ag/AgCl electrode as reference electrode. Potentiodynamic functionalization was achieved by submitting the sample to cyclic voltammetry in a 0.1 M $HClO_4$ solution containing 1 mM of the

respective amino-benzoic acid (2-ABA or 4-ABA), where the potential was scanned between 0 and 1.1 V (vs. Ag/AgCl) at different scan rates.

2.3. Structural, chemical and electrochemical characterization

The structure of the prepared materials was studied by XRD using Cu-Kα radiation at 30 kV and 20 mA. The surface composition and oxidation states of the species in the materials were studied by X-ray photoelectron spectroscopy (XPS) (X-ray photoelectron spectrometer JEOL, JPS-9200) using Mg Kα radiation at 12 kV and 25 mA. Temperature programmed desorption (TPD) experiments were carried out in a DSC-TGA equipment (TA Instruments, SDT 2960 Simultaneous) coupled to a mass spectrometer (Thermostar, Balzers, GSD 300 T3). The thermobalance was purged for 2 h under a helium flow rate of 100 ml min^{-1} and then heated up to 950 °C (heating rate 20 °C min^{-1}).

Fourier Transform Infrared Spectroscopy (FTIR) was used to verify the functionalization process. The samples were dried at 100 ºC for 12 h prior to the experiments. The spectra were recorded between 4000 and 600 cm^{-1} using an IR spectrometer (JASCO FT/IR-4100) with a MCT detector.

The electrochemical characterization of the electrodes was performed using the same standard three-electrode cell configuration already described. The modified electrode was used as working electrode. Two aqueous electrolytes with different pH were used: acid (1M H_2SO_4) and basic media (0.1 M KOH). Prior to the measurements, the electrodes that were electro-modified in 0.1M $HClO_4$ were rinsed in ultrapure water for 5 h and soaked in the corresponding electrolyte for 24 h. The electrochemical behavior was studied by cyclic voltammetry (CV) between -0.2 and 0.8 V (vs. Ag/AgCl) for H_2SO_4, and -0.9 and 0.1 V (vs. Ag/AgCl) for KOH at different scan rates, from 1 to 100 mV s^{-1}. In order to analyze the effect of the functionalization procedure in the conductivity of the materials, measurements of electrochemical impedance spectroscopy (EIS) were performed in the same system described above, before and after the electrochemical modification and the rate performance study. Impedance spectra were measured

at the initial open circuit potential in the frequency range of 10 mHz to 100 kHz with an amplitude voltage of 10 mV.

3. RESULTS AND DISCUSSION

3.1. Electrochemical behavior of ZTC in 0.1M $HClO_4$

Prior to the electrochemical functionalization experiments, a CV run in absence of any ABA monomer in the solution was performed in the electrolyte of choice for understanding the behavior of the ZTC under these conditions. ZTC shows a large oxidation current above 0.6 V in the first anodic scan (Fig. 1a). This fact has been already reported in the literature [5], [29] and is related to the oxidation of the ZTC, which is highly reactive because of a large number of edge sites [5], leading to a direct electro-oxidation mechanism upon positive polarization in acid media. The subsequent cycles show that the oxidation current decreases. At the end of the process it is possible to observe new redox processes at about 0.30 to 0.40 V that are attributed to formation of quinone groups over the ZTC surface which were introduced during the oxidation process [4], Thus, this experiment confirms that ZTC is easily electrochemically oxidized in this electrolyte even using low potentials.

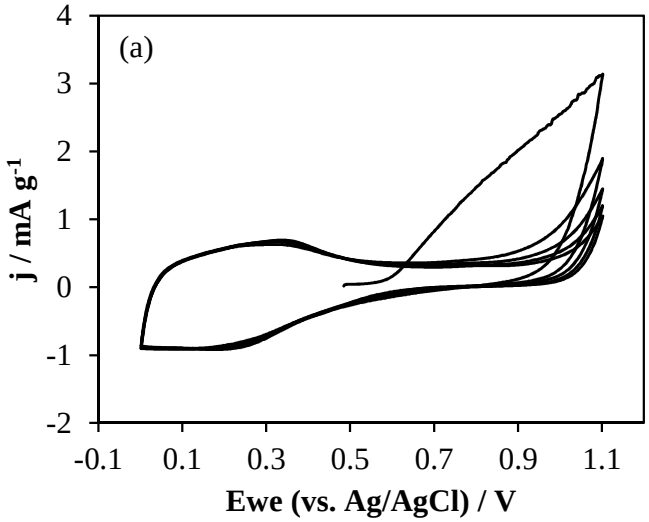

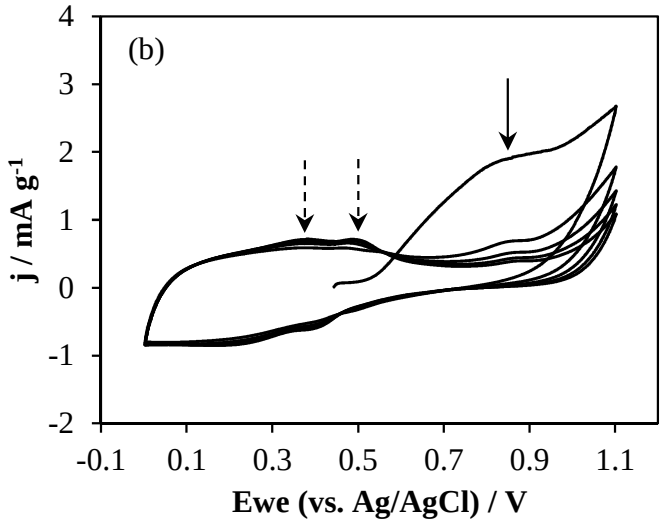

Fig 1. Cyclic voltammetry of an electrode of ZTC in (a) 0.1M $HClO_4$ and (b) 0.1M $HClO_4$ + 1mM 4-ABA at 1 mV s^{-1}, 5 cycles.

3.2. Direct-potentiodynamic electrochemical functionalization of ZTC up to 1.1 V

Fig. 1b shows the CV of the experiment using the 4-ABA in the solution and a potential window from 0 to 1.1 V at 1 mV s^{-1}. The peak corresponding to the amine oxidation clearly appears at 0.84 V (marked by a solid arrow, Fig. 1b), and decreases with the number of cycles [8], [30], as well as the oxidation current at higher potentials. It can also be observed that after the first cycle, several redox processes appear at 0.35 and 0.5 V (dashed arrows, Fig. 1b), which increase with the number of cycles. It is important to note that, in spite of the well-known tendency of ZTC to be electrochemically oxidized through a direct mechanism in acid media [4], [29], leading to the formation of electroactive surface oxygen groups, the redox peaks obtained in the presence of 4-ABA after the first positive scans are found at different potentials, and therefore are expected to come from a different origin. Moreover, the total irreversible charge measured after this electrochemical treatment is different when it is conducted in the presence of 4-ABA, being 56 C g^{-1} higher when the aminobenzoic acid is added in the working electrolyte. Since the amount of charge is larger than that consumed during the direct electrochemical oxidation of ZTC (blank experiment), some charge is being used in the oxidation of the 4-ABA monomers. The activated monomers could then be attached directly to

the surface of ZTC (covalent functionalization) or form 4-ABA oligomers, potentially rendering non-covalent functionalization. This result seems to confirm that ZTC surface can be functionalized using this electrochemical treatment.

3.3. Step-wise-potentiodynamic electrochemical functionalization of ZTC

In order to define the optimal conditions to functionalize ZTC, several conditions were tested with 4-ABA. The experiments were done by using cyclic voltammetry at a higher scan rate (5 mV s^{-1}) in $HClO_4$ + 1 mM of 4-ABA and increasing the more positive potential to higher values from 0.6 to 1.1 V. Fig. 2 shows the voltammograms corresponding to those experiments. It can be observed that initially, there is no oxidation current using a positive potential of 0.6 V. In contrast, when higher potentials are applied, an irreversible oxidation current appears, which is followed by an increase of the area enclosed by the CV. It is also evident that the irreversible oxidation current decreases with the cycles, which points out the depletion of reactive sites from the ZTC surface. Thus, the intensity in the 0-0.6 V region gradually increases when the higher potential is stepped in the positive side up to 0.8 V, 1.0 V and 1.1 V. The increase of the voltammetric charge seems to be related to the formation of slightly irreversible redox processes, being these worse defined than in the experiment in Fig. 1b due to the use of a higher scan rate.

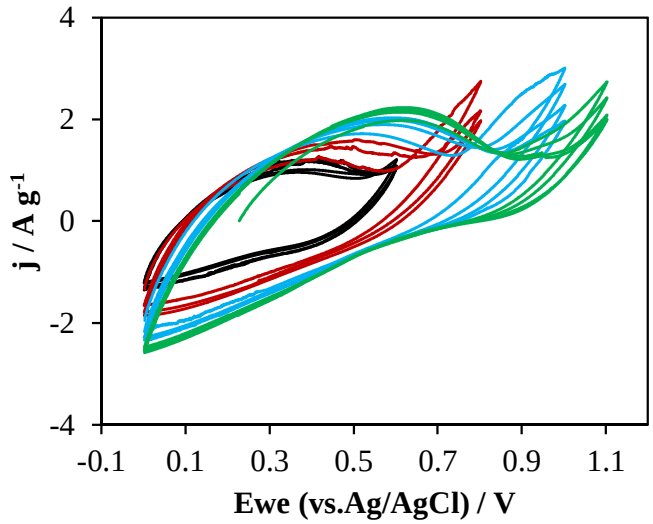

Fig 2. Cyclic voltammetry of an electrode of ZTC in 0.1M $HClO_4$ + 1mM 4-ABA solution at 5 mV s^{-1}. 4 cycles in each positive potential.

3.4. Electrochemical behavior of the initial 4-ABA modified electrodes

For a better resolution of the redox processes resulting from the formation of ABA-related electroactive species, Fig. 3 shows the electrochemical behavior in 1M H_2SO_4 solution of the electrode obtained after step-wise functionalization (the treatment shown in Fig. 2). The areas obtained from the cyclic voltammetry experiments are very similar in all samples. This indicates that the accessible porosity is similar before and after the functionalization process. The CV of 4-ABA functionalized ZTC (ZTC_4-ABA) displays the formation of a well-defined redox process at 0.49 V and a very broad peak at lower potentials (0-0.5 V). The broad peak centered ca. 0.3 V mainly corresponds to the pseudocapacitive contribution of electroactive surface oxygen groups, which are known to be generated during the functionalization process in acid media when potentials higher than 0.8 V are used [5]. This is also observed in the experiment in the absence of ABA, where a broad redox process appears at about 0.30 to 0.40 V that is attributed to the formation of quinone groups over the ZTC surface. Furthermore, if the CV is examined closely, new redox contributions can be found at 0.10 V and 0.35 V (see arrows in Fig. 3). These small redox peaks were not found in previous studies with different carbon materials [8], [30], and seem to be characteristic of the electrochemical functionalization of ZTC with ABA molecules. The peak at 0.49 V is related to the formation of oligomers of 4-ABA, by the incorporation of p-aminobenzoic monomers at the ortho- position to the carboxylic groups, which probably are strongly attached to the ZTC surface through non-covalent interactions, generating electroactive species in acid medium thanks to the protonation reaction of the amino group [31]. The potential value where this redox reaction appears is also very similar to that obtained over CNT for the same electrochemical treatment of functionalization with para-substituted amino-benzene acids [8].

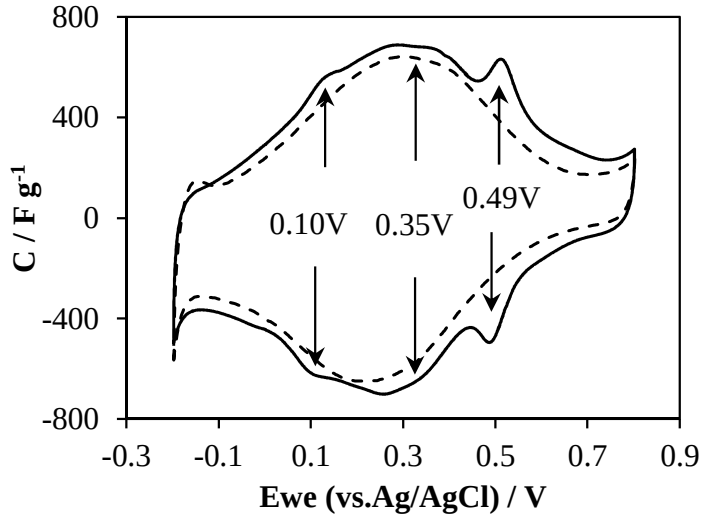

Fig 3. Cyclic voltammetry in 1M H_2SO_4 solution of the functionalized electrodes with 4-ABA (solid line) and without 4-ABA (dashed line) by the electrochemical treatment shown in Fig. 2. Scan rate: 5 mV s^{-1}, 4^{th} cycle.

The characterization in H_2SO_4 of the functionalized electrode by direct potentiodynamic functionalization up to 1.1 V (the treatment shown in Fig. 1) is presented in Fig. 4. It can be observed a very different response compared to the one obtained in Fig. 3. It shows a large peak at 0.38V and a small one at 0.49 V. The last one has been observed before for 4-ABA step-wise functionalized ZTC in Fig. 3, but now the much lower intensity seems to point out that scanning the potential directly to 1.1 V while also using a lower scan rate leaded to the preferential oxidation of the ZTC instead of the formation of the 4-ABA oligomers. This is confirmed by the very similar CV obtained in sulfuric acid 1M of the ZTC treated in perchloric acid in the absence of 4-ABA (dashed line in Fig. 4). In both cases, the main contributions to the pseudocapacitance are the redox processes coming from the electro-generated surface oxygen groups.

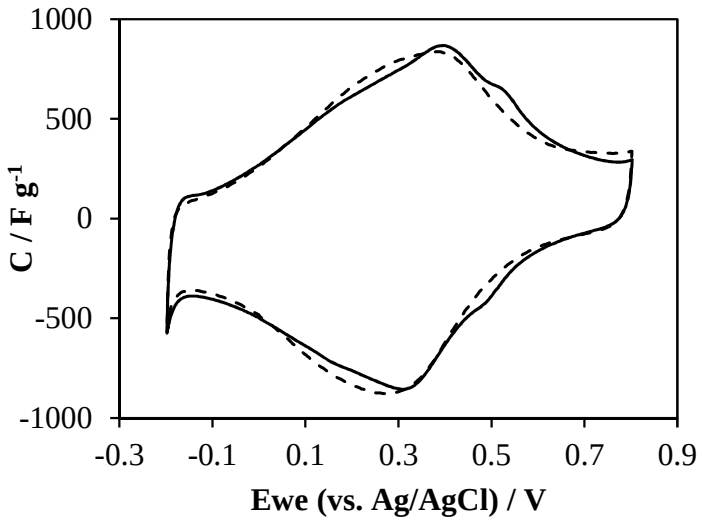

Fig 4. Cyclic voltammetry of the modified electrodes with 4-ABA (solid line) and without 4-ABA (dashed line) in 1M H_2SO_4 solution at 5 mV s^{-1}, 4^{th} cycle.

Consequently, these tests show that the functionalization process depends on the positive potential limit and the scan rate applied during the treatment. When a step-wise process is used with low positive potentials, the 4-ABA related reactions are probably occurring at the same time as the electrochemical oxidation of ZTC. However, at high potentials the electrochemical oxidation of ZTC prevails. Then, if the ZTC electrode is electrochemically treated at low positive potentials before opening the potential window on the positive side, the 4-ABA related electroactive species created on the ZTC surface can hinder the electrooxidation process that would otherwise take part over ZTC surface when it is later exposed to the potential of 1.1 V. Therefore, a lower positive potential limit and short oxidation times (i.e higher scan rate) are preferred in order to promote the 4-ABA functionalization upon the ZTC electrochemical oxidation.

3.5. Optimized electrochemical functionalization of ZTC with aminobenzoic acids

Based on the results shown above, new conditions were chosen. As it was demonstrated before, high positive potentials lead to the oxidation of the ZTC instead of the functionalization, then functionalization treatments until 0.8 V at 5 mV s^{-1} were proposed for 2 and 4-ABA. This potential seems to be high enough to favor the formation of oligomers that will be non-

covalently attached on the surface of ZTC, while direct covalent functionalization will be probably less favored [8], [25]. The results of the functionalization processes are shown in Fig. 5; a blank experiment in which ZTC is submitted to the same treatment, but in the absence of any aminobenzoic acid, is also included for comparison purposes.

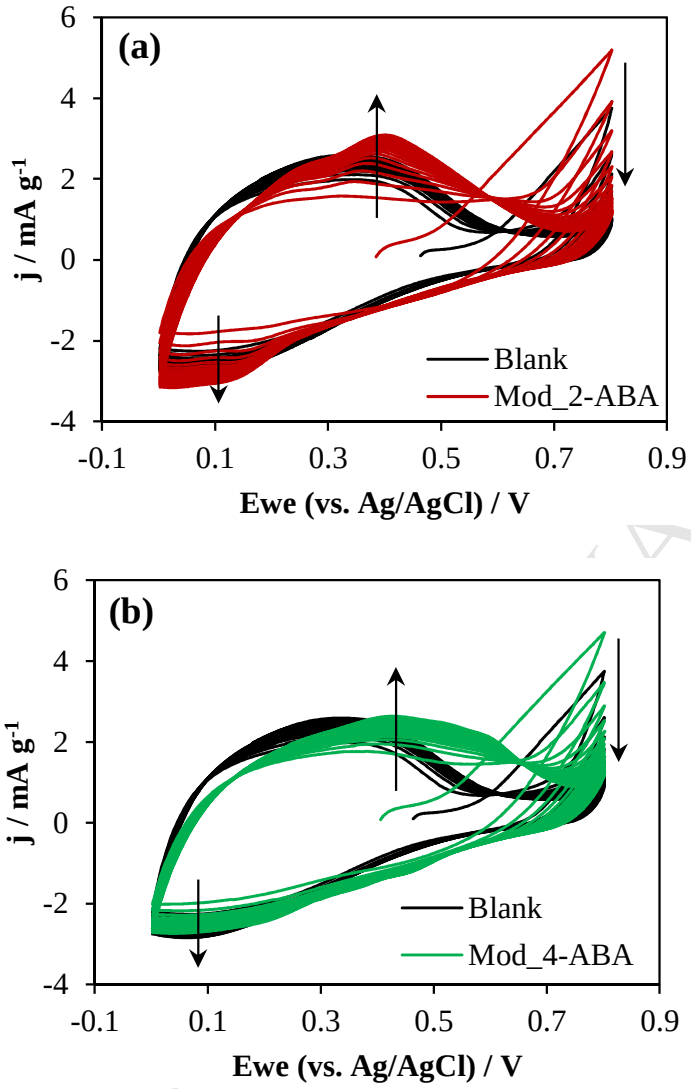

Fig 5. Cyclic voltammetry of an electrode of ZTC in 0.1M $HClO_4$ + (a) 1mM 2-ABA and (b) 1mM 4-ABA at 5 mV s^{-1}, 20 cycles. The black line corresponds to the experiment without monomer in solution.

The results in Fig. 5 do not show a clear peak related to amine oxidation process for 2-ABA and 4-ABA, but compared with the blank experiment, the oxidation current is higher in both cases. Those oxidation currents decrease with the number of cycles, generating redox processes at

lower potentials, being clearer and better defined in the case of the 2-ABA. This result is expected because 2-ABA polymerizes easier than 4-ABA due to steric effects. The 2-ABA is able to form a linear polymer similar to PANI, whereas 4-ABA can form very short-chain ramified oligomers [31].

Fig. 6 shows the characterization of these functionalized ZTC electrodes with 2-ABA (ZTC_2ABA) and 4-ABA (ZTC_4ABA) in acid (1M H_2SO_4) and basic (0.1M KOH) media. Compared to the blank experiment (i.e. ZTC electrochemically treated in 0.1M $HClO_4$), the functionalized ZTCs shows unique redox peaks, corresponding to the attached molecules that are electroactive in both media, and the position of the main redox peaks is different for each ABA. In acid medium (Fig. 6a), the ZTC_2ABA shows the formation of three peaks at 0.11, 0.27 and 0.35 V. The peaks appear at lower potentials than the ZTC_4ABA, which shows redox processes at 0.35 and 0.51 V. This fact can be attributed to the self-doping effect of the carboxylic group close to the amine group [31].

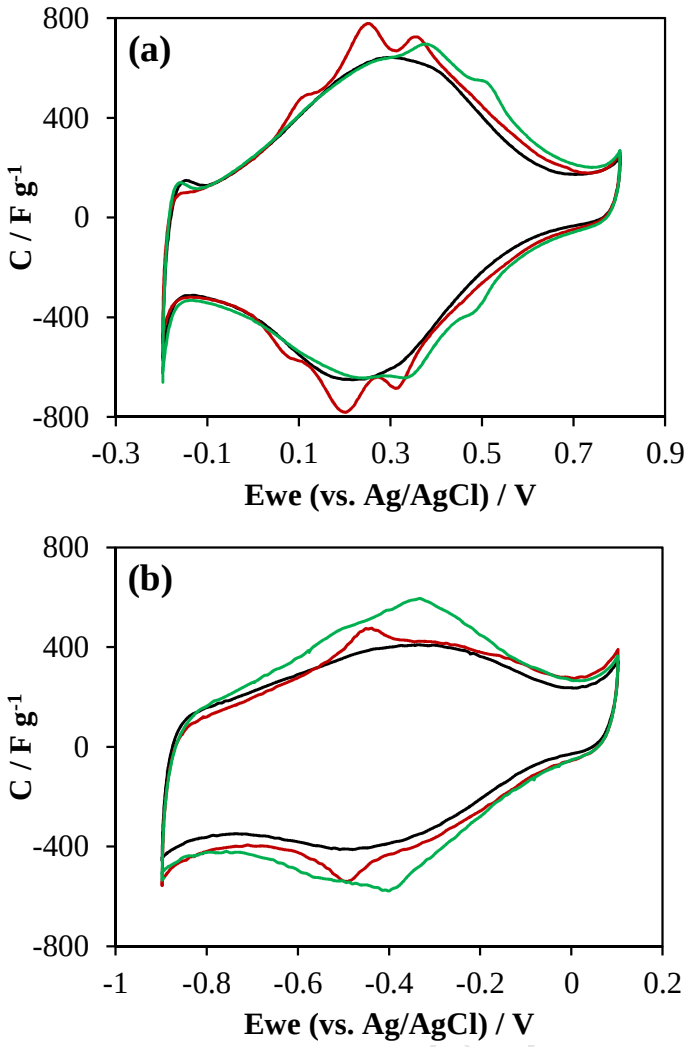

Fig 6. Cyclic voltammetry of functionalized ZTC without ABA (black line), with 2-ABA (red line) and 4-ABA (green line) in (a) 1M H_2SO_4 and (b) 0.1M KOH at 5 mVs^{-1}, 4^{th} cycle.

The CV response in basic medium (Fig. 6b) is different to that in acid medium. In the case of ZTC_2-ABA, only a small redox process at -0.45 V appears, which is close to the potential where the peak of ZTC_2-ABA is found in 1M H_2SO_4 (Fig. 6a). Except for that redox process, the electrode behaves fairly similar to the modified ZTC in the absence of any ABA (black line in Fig. 6b), which shows less intense processes than in acid electrolyte in this potential window. Interestingly, for the ZTC_4-ABA electrode two broad peaks centered at -0.55 and -0.30 V appear which provide to this sample with a higher contribution of pseudocapacitance in this electrolyte. The 2-ABA polymer is known to be partially soluble in basic media, and therefore it could be detached from ZTC surface and washed out from the porosity in 0.1 M KOH solution.

In spite of that, it is possible to see remaining redox processes, pointing out that part of the 2-ABA functionalities (probably those covalently bonded) still remain attached to the surface. The higher stability and electroactivity showed by ZTC_4-ABA could be explained considering that ZTC has been covalently modified in a larger extent because the polymer formation with this molecule is more impeded.

In general, the materials show a net increase in the capacitance, as consequence of the pseudocapacitance contribution of the redox processes associated to the ABA molecules. Capacitances in acid medium of 399 F g^{-1} were measured at 1 mV s^{-1} for the ZTC treated in the absence of ABA, whereas values of 427 and 441 F g^{-1} were obtained for ZTC_2-ABA and ZTC_4-ABA at the same scan rate, respectively. When the capacitance is determined in basic medium, it varies to 286, 318 and 364 F g^{-1} for the blank, ZTC_2-ABA and ZTC_4-ABA. Fig. 7 shows the rate performance for all samples in acid and basic media. Interestingly, the net increase in capacitance, which is as high as 78 F g^{-1} for ZTC_4-ABA in basic medium and 30-35 F g^{-1} for both functionalized electrodes in acid medium, is kept upon increasing the scan rate; this demonstrates that the ABA polymers and molecules must be attached on the carbon surface, and therefore the electron transfer and charge propagation to ZTC is fast, unlike a solution redox process.

If we consider that each redox process is related to the presence of one electroactive heteroatom and only implies the transfer of one electron, the amount of heteroatoms functionalized on the ZTC surface can be determined from the differences in charge registered during the CV measurements between the electrochemically functionalized ZTC in the absence and presence of ABA. From the results obtained in acid media, where all the introduced functionalities should be electroactive, the amounts are 0.416 and 0.368 mmol g^{-1} for ZTC_2-ABA and ZTC_4-ABA, respectively. The capacitance retention at fast scan rates is higher in acid medium and better than for the oxidized ZTC, which could be helpful for high power applications. In both media, the loss of capacitance seems to be mainly inherent to ZTC and unaffected by the presence of the functionalities.

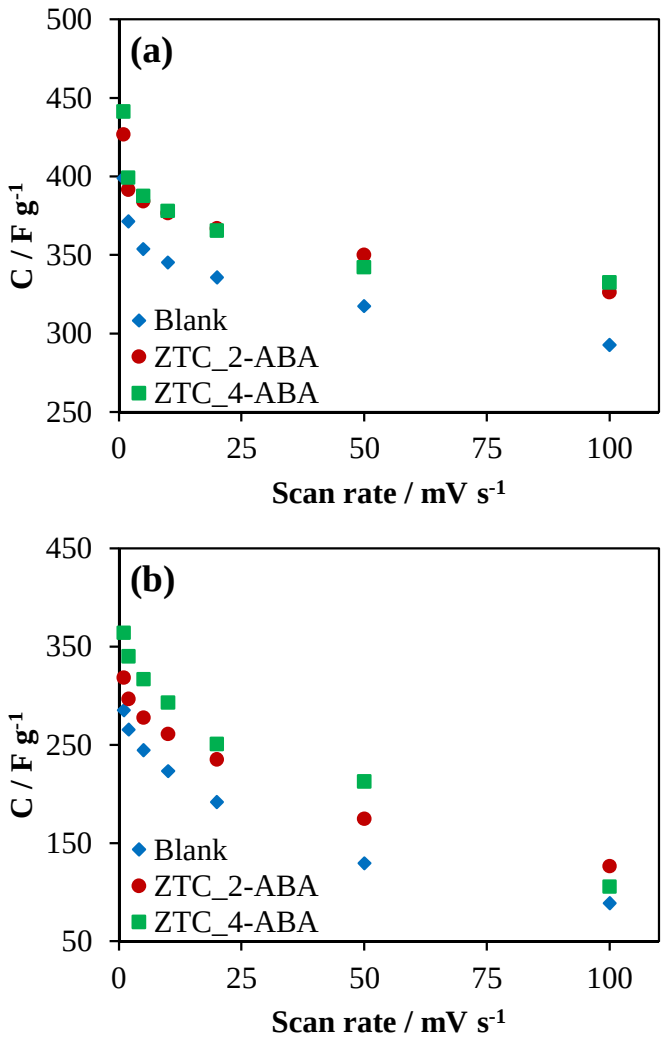

Fig 7. Rate performance of functionalized ZTC in (a) 1M H_2SO_4 and (b) 0.1M KOH.

The possible effect of these ABA species on the conductivity and ion mobility of the electrode has been analyzed by EIS. Fig. 8 shows the Nyquist plot of the ZTC in 0.1M perchloric acid before and after the functionalization with 2-ABA. It is possible to see that the electrodes show the characteristic response of a porous carbon electrode and that, after the functionalization, a similar trend is observed in both cases. First, the Equivalent Series Resistance (ESR) seems to be slightly improved after the electrochemical treatment, without any relevant differences arising in the size of their semicircle after the functionalization. Second, a rather low Equivalent Distributed Resistance (EDR, a known feature of ZTC, which possesses a highly interconnected array of micropores that enhances ion mobility through it) and the quasi-ideal capacitor behavior with a vertical line recorded at low frequencies, are kept after the electrochemical

treatment in 0.1 M $HClO_4$, independently of the presence of ABA in the electrolyte. The similar tendencies found seem to confirm that the formation of ABA functionalities in the pore network of ZTC do not render a significant decrease neither in electrical conductivity nor in ion mobility which allow to preserve a good retention of capacitance (Fig. 7).

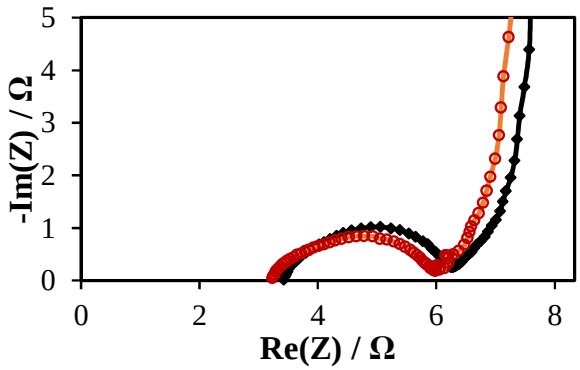

Fig 8. Nyquist plot of the pristine (black line) and 2-ABA modified electrode (red line) in 0.1M $HClO_4$.

3.6. Electrochemical stability of the electrodes

In order to evaluate the electrochemical stability of the modified ZTC materials, cyclability tests were done in acid electrolyte (1M H_2SO_4). Fig. 9 shows the results of CV at 10 mV s^{-1} after the 1st and 500th cycle. It can be seen that the CV shows an excellent stability after cycling in both cases. This result confirms that the redox processes are not occurring in solution (otherwise, the products will diffuse out the porosity towards the bulk of the solution) and correspond to redox-active species strongly attached to the surface of the electrode material.

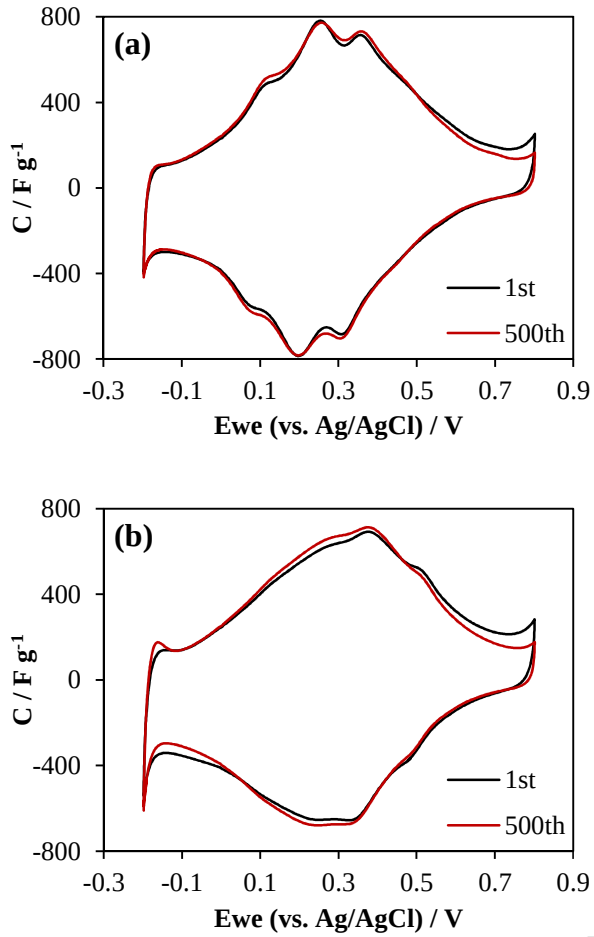

Fig 9. Cyclic voltammetry in 1M H_2SO_4 of (a) ZTC_2-ABA and (b) ZTC_4-ABA, at 10 mVs^{-1}.

The behavior of the functionalized electrodes at very high positive potentials was tested by performing a CV from 0 to 1.2 V in 1M H_2SO_4 at 5 mV s^{-1}, 5 cycles. Fig. 10 shows the CV obtained in the characterization potential region for the three electrodes after the treatment. It is possible to observe significant changes in the CV after subjecting the materials to strong oxidation conditions. The CVs patterns of the modified ZTC samples are quite similar to the sample without any ABA functionalities. Interestingly, the electrode ZTC_4-ABA still shows the unique redox peak at 0.51 V, which corresponds to electroactive species. It seems that such high potentials are oxidizing and removing most of the ABA species present on the ZTC, being the most stable those derived from 4-ABA.

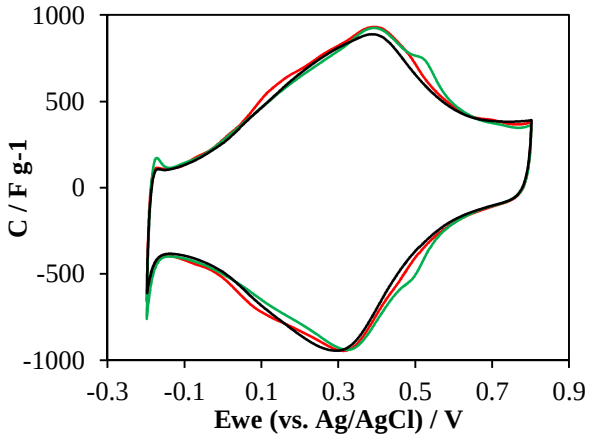

Fig 10. Cyclic voltammetry in 1M H_2SO_4 after oxidation treatment of functionalized ZTC without ABA (black line) and with 2-ABA (red line) and 4-ABA (green line) at 5 mV s^{-1}, 5^{th} cycle.

3.7. Structural and chemical characterization

X-ray diffraction patterns of ZTC are shown in Fig. 11a. The small peak displayed at 2θ = 18.2º correspond to the PTFE used during the fabrication of the ZTC paste. ZTC treated in the absence of ABA molecules (blank experiment) shows a sharp peak at 2θ = 6.4º, being derived from {111} reflections of zeolite Y as a template [28]. ZTC_2-ABA and ZTC_4-ABA show a weaker peak, and also a smaller contribution of the diffraction at low angles. These features can be explained on the basis of the formation of the species inside the pores of the ZTC rather than in a destruction of the ordered structure. Thus, the intensity ratio of the {111} peak with respect to the background intensity at 2θ = 10 º decreased 45 % and 46 % in the case of the ZTC_2-ABA and ZTC_4-ABA, respectively. This ratio is similar to the decrease found in the intensity ratio at low angles. As shown before, the functionalization of ZTC with ABA does not hinder the ion mobility and charge transfer through ZTC in aqueous electrolyte, a result that seems to confirm that the structure of ZTC is not damaged; rather than that, it is filled with the ABA functionalities.

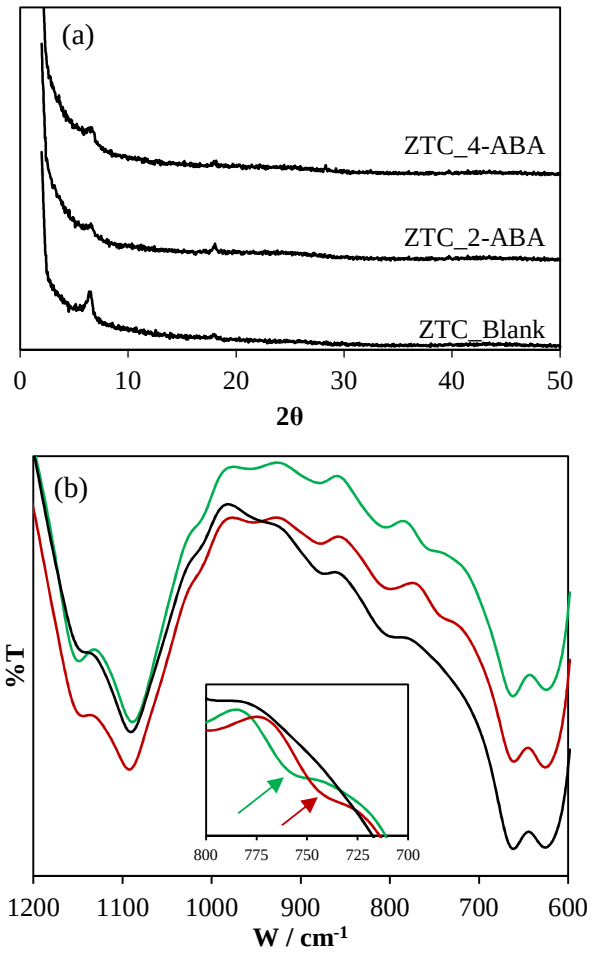

Fig 11. (a) XRD patterns of functionalized ZTC with and without ABA. (b) FTIR spectra of functionalized ZTC without ABA and with 2-ABA (red line), 4-ABA (green line).

Fig. 11b shows the FTIR transmission spectra in the region between 1200 and 600 cm^{-1} of the three electrodes presented before. It is important to note that all bands found for the electrode of ZTC functionalized in the absence of ABA are also present in the ABA-functionalized electrodes, showing no shifting on their position. Most of them can be ascribed to the presence of oxygen groups or to the PTFE binder. A new band approximately at 740 and 760 cm^{-1} can be seen in ZTC_2-ABA and ZTC_4-ABA, respectively, which is not found in the ZTC electrode when no ABA is added during the functionalization treatment. It corresponds to the stretching mode of aromatic amine groups present in the ABA molecule, confirming the successful functionalization of ZTC with the amino-benzoic acids [32], [33]. The position of the band

seems to shift depending on whether the 2- or the 4-ABA monomers are used during the functionalization, which agrees with the different structures that can be obtained with the two monomers.

The surface composition and the oxidation states of the species of the materials were studied by XPS. An increase in nitrogen and oxygen content is observed for all functionalized samples compared with ZTC (Table 1). Blank experiment confirmed that most of the oxygen in the samples is due to the electrooxidation process. However, the additional oxygen content can be attributed to the aminobenzoic molecule that has a carboxylic functionality in its structure. This is also supported with the amount of nitrogen in the functionalized ZTC, which shows an increment that reaches a 1.4% of nitrogen in its atomic composition. It is important to remark that in the case of ZTC_2-ABA the content in nitrogen and oxygen is higher than for the ZTC_4-ABA. The results confirm that the functionalization at lower potentials is higher in the case of 2-ABA than 4-ABA. The results obtained by XPS are in agreement with the ones obtained by electrochemical measurements. The polymerization over ZTC surface is easier for the one with ortho- position; in the case of para- substituted aminobenzoic acid the formation of the polymer is impeded because of the aforementioned steric effects, which leads to the formation of few short-chain oligomers.

Table 1. Atomic composition obtained by XPS of functionalized ZTC without ABA and with 2-ABA and 4-ABA

Sample	**C1s / At.%**	**N1s / At.%**	**O1s / At.%**
ZTC_Blank	94.0	0.0	6.0
ZTC_2-ABA	93.4	1.4	5.2
ZTC_4-ABA	94.5	1.2	4.4

Fig. 12 shows the N1s XPS spectra for the different functionalized ZTC. For both samples, a N1s peak was observed at 400.3 eV, which can be separated in two contributions, one at 399.3 eV assigned to neutral amines, and a second at 400.5 eV assigned to positively charged amines [34]. The presence of these nitrogen species suggests that functionalization was produced by the formation of ramified polymers from the linkage of several aminoacids molecules via amine bridges [31].

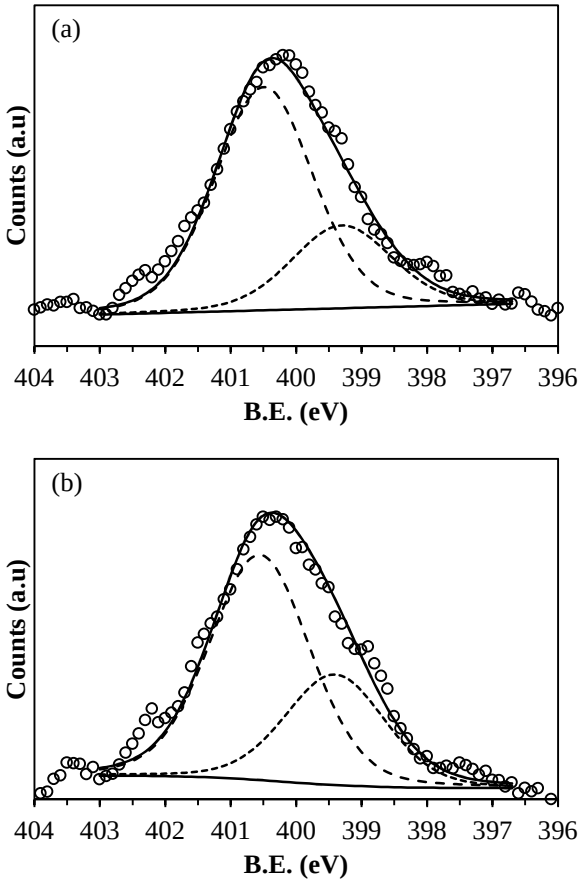

Fig 12. XPS spectra N1s for: (a) ZTC_2ABA, (b) ZTC_4ABA

The formation of nitrogen-rich stable polymers and oligomers was also demonstrated by temperature-programmed desorption (TPD). Fig. 13 shows the TPD profiles for all samples. In the experiments, the evolution of CO, CO_2, HCN and NH_3 was followed. Several other m/z signals related to the formation of other gaseous products (NO, NO_2, methane, hydrogen…) were also followed, but are not shown herein since they did not provide any relevant information. The decomposition of surface oxygen functionalities of a porous carbon upon heating in inert atmosphere is a well-known process that has been extensively used for characterizing the surface functionalities of porous carbon materials [35], [36]. It is known that CO evolution is related to the decomposition of neutral and basic groups such as carbonyl, quinones, phenols, ethers and some others, which can be identified thanks to their different thermal stabilities, which causes them to evolve as CO at different temperatures. Similarly, CO_2 desorption is mainly related to the decomposition of carboxylic, anhydride and lactone moieties; in the case of anhydrides, they are also accompanied by the release of a CO molecule for each

formed CO_2 molecule. Similarly, the presence of N-functionalities can also be detected following the m/z lines corresponding to the gases evolved during its decomposition [37].

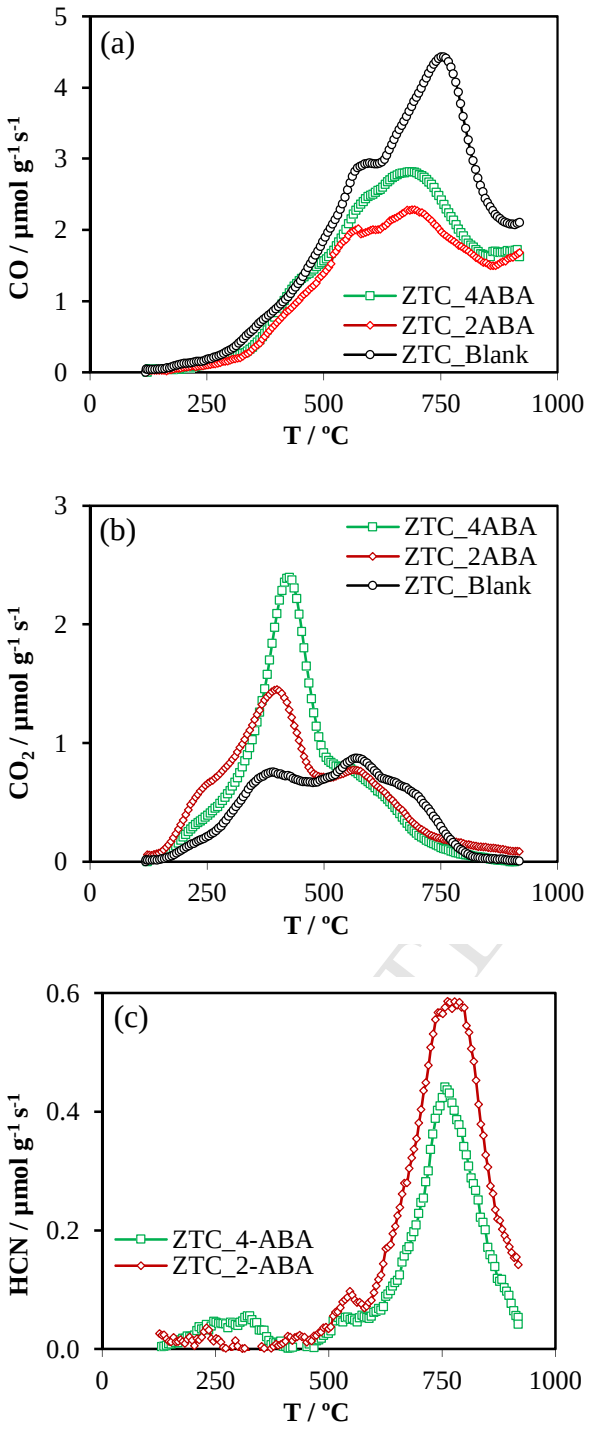

Fig 13. TPD profiles for the ZTC, ZTC_2-ABA y ZTC_4-ABA electrodes (a) CO, (b) CO_2 and (c) HCN evolution

The CO-TPD profiles in Fig. 13a show that the three electrodes have a large amount of surface oxygen groups, though the nature and amount of CO-evolving groups are quite different for the ZTC sample after the electrochemical treatment in the absence of ABA (ZTC_Blank). A large peak of CO desorption at 750 ºC can be seen for this electrode. This seems to be related to the decomposition of quinone/carbonyl type groups, which are known to be formed during the electrochemical oxidation of ZTC [4]. Interestingly, the amount of CO-type groups is much smaller in the case of the ZTC_2-ABA and ZTC_4-ABA and the most predominant contribution is a peak at around 650 ºC, being associated to decomposition of less thermally stable groups. These results show that, as previously discussed, during the functionalization treatment in the presence of ABA molecules most of the charge is used for the ABA oxidation thus preventing the ZTC electrochemical oxidation. Probably, either the ABA-containing molecules occupy the ZTC active sites or the ABA-related reactions are faster than the ZTC electrooxidation.

It is important to highlight here that quinone/carbonyl groups have been claimed to be electroactive specially in acid electrolyte [38], and are clearly observed in the case of ZTC [5], [29]. However, the pseudocapacitance contribution associated to redox reactions of quinone-type groups was similar for the ABA-modified samples (see Fig. 6). Therefore, it can be concluded that not all the CO-type surface oxygen groups that are formed during the electrochemical functionalization of ZTC are electroactive, in agreement with previous observations [39], and that most of the electroactive oxygen groups are still present after functionalization with ABA molecules, thus suggesting that overoxidation of the carbon material can be avoided when ABA monomers are added during the treatment. This opens the possibility of increasing the selectivity towards the most electroactive surface functional groups.

Another interesting result comes from the examination of the CO_2 profiles (Fig. 13b). They show an increase of CO_2 desorption at around 400 ºC in the ABA-functionalized ZTC. The narrow desorption peaks correspond to the thermal decomposition of a homogeneous species. It clearly corresponds to the decomposition of the carboxylic acid from the ABA oligomers. The CO_2 evolution observed for ZTC_2-ABA, contains a CO_2-peak at lower temperatures that can

be due to the destabilizing effect of the amine bridge in the vicinity of the carboxylic group, facilitating its thermal decomposition.

Fig. 13c shows the HCN-TPD profiles of the ABA-functionalized ZTC electrodes. The profile of ZTC functionalized in absence of any ABA molecule was subtracted to those shown to rule out the possible interference of the PTFE used during the fabrication of the ZTC paste (which also has a contribution in the m/z=27 line) in this experiment. Desorption of HCN forms a large peak at 750 ºC, and the release of small amounts of NH_3 was also found at this temperature (not shown). This process seems to be connected to the thermal decomposition of the amine and imine groups that exist in the oligomers, polymers and other species obtained from functionalization in the presence of 2- and 4-ABA.

The quantification of the amount of desorbed CO, CO_2, NH_3 and HCN is included in Table 2. It is important to remark that the quantity of HCN for ZTC_2-ABA is twice that of ZTC_4-ABA, which confirms that 2-ABA is more easily polymerized than 4-ABA. The relationship between the amount of N-containing groups and the amount of carboxylic groups (determined from difference with the blank experiment) seems to be close to 1:1 in both cases. Another interesting result is the clear inverse relationship between the amount of N groups and the amount of CO-desorbing groups. The larger the amount of N groups (i.e. the more extensive the functionalization is), the lower the amount of electrochemically generated CO groups. Moreover, the amount of electroactive groups that were measured from the charge in the CVs of Fig. 6 (416 and 368 µmol g^{-1} for 2- and 4-ABA, respectively) seems to be in agreement with the amount of N groups.

Table 2. Evolution of CO, CO_2, HCN and NH_3 from TPD experiments

	CO µmol g^{-1}	**CO_2 µmol g^{-1}**	**HCN µmol g^{-1}**	**NH_3 µmol g^{-1}**
ZTC_2ABA	2829	1361	295	114
ZTC_4ABA	3332	1457	170	109
ZTC_Blank	4529	1022	0	0

4. CONCLUSIONS

The electrochemical functionalization of ZTC with 2- and 4- aminobenzoic acids has been carried out using a potentiodynamic method. The functionalization was achieved by using oxidative conditions where the amino group of the amino-benzoic acid is activated and can form either an electroactive polymer layer on the top of the ZTC surface or a covalent bond with the highly abundant edge sites of ZTC. Different experimental conditions were tested in order to perform a successful functionalization. When a high upper potential limit is used (1.1 V), the generation of oxygen functionalities is preferred over the functionalization with aminobenzene acids. This is due to the low amount of monomer and the high reactivity of ZTC and high concentration of edge sites. Consequently, the functionalization process was proposed and successfully achieved using lower upper potential (0.8 V). The electrochemical behavior of the functionalized samples have been carried out in acid and basic media, demonstrating the appearance of redox processes, some of them being unique to this system and being probably related to the collaboration between surface functionalities of the highly reactive ZTC and ABA-derived short chain polymers. Thus, the functionalized electrodes show an increase in the capacitance value compared to the pristine one due to the pseudocapacitance contribution. The increase in capacitance is also maintained at high scan rates, pointing out a fast charge transfer between the inserted functionalities and the ZTC electrode. The introduced functionalities are stable upon successive cycling and exposure to high oxidative potentials leads to an oxidation and removal of most of the ABA species present on the ZTC surface. XRD confirmed that functionalities have been generated inside the porosity of ZTC, while FTIR, XPS and TPD experiments verified the functionalization process by confirming the presence of different nitrogen groups over the ZTC surface. These promising results show an alternative method for the modification of surface chemistry of highly porous carbon materials.

ACKNOWLEDGEMENTS

The authors would like to thank MINECO and FEDER (CTQ2012/31762, MAT2013-42007-P and PRI-PIBJP-2011-0766), Generalitat Valenciana (PROMETEO/2013/038 and PROMETEOII/2014/010) for the financial support. RRR thanks MINECO for a 'Juan de la Cierva' contract (JCI-2012-12664). CGG gratefully acknowledges Generalitat Valenciana for the financial support through a Santiago Grisolía grant (GRISOLIA/2013/005). This work is also supported by the Nano-Macro Materials, Devices and System Research Alliance and by Network Joint Research Center for Materials and Devices. The authors thank Dr. Alberto Castro-Muñiz for his help in the XPS measurements.

REFERENCES

[1] H. Nishihara and T. Kyotani, "Templated nanocarbons for energy storage," *Adv. Mater.*, vol. 24, no. 33, pp. 4473–4498, 2012.

[2] T. Kyotani, Z. Ma, and A. Tomita, "Template synthesis of novel porous carbons using various types of zeolites," *Carbon*, vol. 41, no. 7, pp. 1451–1459, 2003.

[3] H. Nishihara, Q.-H. Yang, P.-X. Hou, M. Unno, S. Yamauchi, R. Saito, et al, "A possible buckybowl-like structure of zeolite templated carbon," *Carbon*, vol. 47, no. 5, pp. 1220–1230, 2009.

[4] R. Berenguer, H. Nishihara, H. Itoi, T. Ishii, E. Morallón, D. Cazorla-Amorós, et al, "Electrochemical generation of oxygen-containing groups in an ordered microporous zeolite-templated carbon," *Carbon*, vol. 54, pp. 94–104, 2013.

[5] H. Itoi, H. Nishihara, T. Ishii, K. Nueangnoraj, R. Berenguer, and T. Kyotani, "Large Pseudocapacitance in Quinone-Functionalized Zeolite-Templated Carbon," *Bull. Chem. Soc. Jpn.*, vol. 87, no. 2, pp. 250–257, 2014.

[6] R. Berenguer, J. P. Marco-Lozar, C. Quijada, D. Cazorla-Amorós, and E. Morallón, "A comparison between oxidation of activated carbon by electrochemical and chemical treatments," *Carbon*, vol. 50, no. 3, pp. 1123–1134, 2012.

[7] S. Maldonado and K. J. Stevenson, "Influence of nitrogen doping on oxygen reduction electrocatalysis at carbon nanofiber electrodes.," *J. Phys. Chem. B*, vol. 109, no. 10, pp. 4707–16, 2005.

[8] C. González-Gaitán, R. Ruiz-Rosas, E. Morallón, and D. Cazorla-Amorós, "Functionalization of carbon nanotubes using aminobenzene acids and electrochemical methods. Electroactivity for the oxygen reduction reaction," *Int. J. Hydrogen Energy*, vol. 40, no. 34, pp. 11242–11253, 2015.

[9] D. Salinas-Torres, S. Shiraishi, E. Morallón, and D. Cazorla-Amorós, "Improvement of carbon materials performance by nitrogen functional groups in electrochemical capacitors in organic electrolyte at severe conditions," *Carbon*, vol. 82, pp. 205–213, 2015.

[10] O. Ornelas, J. M. Sieben, R. Ruiz-Rosas, E. Morallón, D. Cazorla-Amorós, J. Geng, et al, "On the origin of the high capacitance of nitrogen-containing carbon nanotubes in acidic and alkaline electrolytes.," *Chem. Commun.*, vol. 50, no. 77, pp. 11343–6, 2014.

[11] D. Salinas-Torres, O. Ornelas, R. Ruiz-Rosas, D. Cazorla-Amorós, and E. Morallón, "Almacenamiento de energía eléctrica en materiales carbonosos," in *Desarrollo y aplicaciones de materiales avanzados de carbón*, F. Carrasco Marín, F. J. Maldonado Hódar, and M. Á. Álvarez Merino, Eds. Universidad Internacional de Andalucía, 2014, p. 428.

[12] E. Raymundo-Piñero, D. Cazorla-Amorós, and A. Linares-Solano, "The role of different nitrogen functional groups on the removal of SO2 from flue gases by N-doped activated carbon powders and fibres," *Carbon*, vol. 41, no. 10, pp. 1925–1932, 2003.

[13] L. F. Mabena, S. Sinha Ray, S. D. Mhlanga, and N. J. Coville, "Nitrogen-doped carbon nanotubes as a metal catalyst support," *Appl. Nanosci.*, vol. 1, no. 2, pp. 67–77, 2011.

[14] F. J. Maldonado-Hódar and S. Morales-Torres, "Aplicaciones de los materiales de carbón en catálisis," in *Desarrollo y aplicaciones de materiales avanzados de carbón*, F. Carrasco Marín, F. J. Maldonado Hódar, and M. Á. Álvarez Merino, Eds. Universidad Internacional de Andalucía, 2014, p. 428.

[15] Y. Wang, Y. Shao, D. W. Matson, J. Li, and Y. Lin, "Nitrogen-doped graphene and its application in electrochemical biosensing.," *ACS Nano*, vol. 4, no. 4, pp. 1790–8, 2010.

[16] P.-X. Hou, H. Orikasa, T. Yamazaki, K. Matsuoka, A. Tomita, N. Setoyama, et al, "Synthesis of Nitrogen-Containing Microporous Carbon with a Highly Ordered Structure and Effect of Nitrogen Doping on H_2O Adsorption," *Chem. Mater.*, vol. 17, no. 20, pp. 5187–5193, 2005.

[17] C. O. Ania, V. Khomenko, E. Raymundo-Piñero, J. B. Parra, and F. Béguin, "The Large Electrochemical Capacitance of Microporous Doped Carbon Obtained by Using a Zeolite Template," *Adv. Funct. Mater.*, vol. 17, no. 11, pp. 1828–1836, 2007.

[18] Z. Yang, Y. Xia, X. Sun, and R. Mokaya, "Preparation and Hydrogen Storage Properties of Zeolite-Templated Carbon Materials Nanocast via Chemical Vapor Deposition: Effect of the Zeolite Template and Nitrogen Doping," *J. Phys. Chem. B*, vol. 110, no. 37, pp. 18424–18431, 2006.

[19] Y. Xia, G. S. Walker, D. M. Grant, and R. Mokaya, "Hydrogen storage in high surface area carbons: experimental demonstration of the effects of nitrogen doping.," *J. Am. Chem. Soc.*, vol. 131, no. 45, pp. 16493–9, 2009.

[20] H. Nishihara, P.-X. Hou, L.-X. Li, M. Ito, M. Uchiyama, T. Kaburagi, et al, "High-Pressure Hydrogen Storage in Zeolite-Templated Carbon," *J. Phys. Chem. C*, vol. 113, no. 8, pp. 3189–3196, 2009.

[21] R. Ruiz-Rosas, M. J. Valero-Romero, D. Salinas-Torres, J. Rodríguez-Mirasol, T. Cordero, E. Morallón, et al, "Electrochemical performance of hierarchical porous carbon materials obtained from the infiltration of lignin into zeolite templates," *ChemSusChem*, vol. 7, no. 5, pp. 1458–67, 2014.

[22] M. J. Mostazo-López, R. Ruiz-Rosas, E. Morallón, and D. Cazorla-Amorós, "Generation of nitrogen functionalities on activated carbons by amidation reactions and Hofmann rearrangement: Chemical and electrochemical characterization," *Carbon*, vol. 91, pp. 252–265, 2015.

[23] D. Salinas-Torres, J. M. Sieben, D. Lozano-Castello, E. Morallón, M. Burghammer, C. Riekel, et al, "Characterization of activated carbon fiber/polyaniline materials by position-resolved microbeam small-angle X-ray scattering," *Carbon*, vol. 50, no. 3, pp. 1051–1056, 2012.

[24] D. Salinas-Torres, J. M. Sieben, D. Lozano-Castelló, D. Cazorla-Amorós, and E. Morallón, "Asymmetric hybrid capacitors based on activated carbon and activated carbon fibre–PANI electrodes," *Electrochim. Acta*, vol. 89, pp. 326–333, 2013.

[25] G. Yang, Y. Shen, M. Wang, H. Chen, B. Liu, and S. Dong, "Copper hexacyanoferrate multilayer films on glassy carbon electrode modified with 4-aminobenzoic acid in aqueous solution.," *Talanta*, vol. 68, no. 3, pp. 741–7, 2006.

[26] X. Li, Y. Wan, and C. Sun, "Covalent modification of a glassy carbon surface by electrochemical oxidation of r-aminobenzene sulfonic acid in aqueous solution," *J. Electroanal. Chem.*, vol. 569, no. 1, pp. 79–87, 2004.

[27] G. Yang, B. Liu, and S. Dong, "Covalent modification of glassy carbon electrode during electrochemical oxidation process of 4-aminobenzylphosphonic acid in aqueous solution," *J. Electroanal. Chem.*, vol. 585, no. 2, pp. 301–305, 2005.

[28] Z. Ma, T. Kyotani, Z. Liu, O. Terasaki, and A. Tomita, "Very High Surface Area Microporous Carbon with a Three-Dimensional Nano-Array Structure: Synthesis and Its Molecular Structure," *Chem. Mater.*, vol. 13, no. 12, pp. 4413–4415, 2001.

[29] K. Nueangnoraj, R. Ruiz-Rosas, H. Nishihara, S. Shiraishi, E. Morallón, D. Cazorla-Amorós, et al, "Carbon–carbon asymmetric aqueous capacitor by pseudocapacitive positive and stable negative electrodes," *Carbon*, vol. 67, pp. 792–794, 2014.

[30] A. Benyoucef, F. Huerta, M. I. Ferrahi, and E. Morallon, "Voltammetric and in situ FT-IRS study of the electropolymerization of o-aminobenzoic acid at gold and graphite carbon electrodes: Influence of pH on the electrochemical behaviour of polymer films," *J. Electroanal. Chem.*, vol. 624, no. 1–2, pp. 245–250, 2008.

[31] A. Benyoucef, F. Huerta, J. L. Vázquez, and E. Morallon, "Synthesis and in situ FTIRS characterization of conducting polymers obtained from aminobenzoic acid isomers at platinum electrodes," *Eur. Polym. J.*, vol. 41, no. 4, pp. 843–852, 2005.

[32] T. Ramanathan, F. T. Fisher, R. S. Ruoff, and L. C. Brinson, "Amino-Functionalized Carbon Nanotubes for Binding to Polymers and Biological Systems," *Chem. Mater.*, vol. 17, no. 6, pp. 1290–1295, 2005.

[33] J. Shen, W. Huang, L. Wu, Y. Hu, and M. Ye, "Study on amino-functionalized multiwalled carbon nanotubes," *Mater. Sci. Eng. A*, vol. 464, no. 1–2, pp. 151–156, 2007.

[34] E. Raymundo-Piñero, D. Cazorla-Amorós, A. Linares-Solano, J. Find, U. Wild, and R. Schlögl, "Structural characterization of N-containing activated carbon fibers prepared from a low softening point petroleum pitch and a melamine resin," *Carbon*, vol. 40, no. 4, pp. 597–608, 2002.

[35] Y. Otake and R. G. Jenkins, "Characterization of oxygen-containing surface complexes created on a microporous carbon by air and nitric acid treatment," *Carbon*, vol. 31, no. 1, pp. 109–121, 1993.

[36] M. C. C. Román-Martínez, D. Cazorla-Amorós, A. Linares-Solano, and C. Salinas-Martínez de Lecea, "TPD and TPR characterization of carbonaceous supports and Pt/C catalysts," *Carbon*, vol. 31, no. 6, pp. 895–902, 1993.

[37] H. F. Gorgulho, J. P. Mesquita, F. Gonçalves, M. F. R. Pereira, and J. L. Figueiredo, "Characterization of the surface chemistry of carbon materials by potentiometric titrations and temperature-programmed desorption," *Carbon*, vol. 46, no. 12, pp. 1544–1555, 2008.

[38] M. J. Bleda-Martínez, J. A. Maciá-Agulló, D. Lozano-Castelló, E. Morallón, D. Cazorla-Amorós, and A. Linares-Solano, "Role of surface chemistry on electric double layer capacitance of carbon materials," *Carbon*, vol. 43, no. 13, pp. 2677–2684, 2005.

[39] S. Leyva-García, K. Nueangnoraj, D. Lozano-Castelló, H. Nishihara, T. Kyotani, E. Morallón, et al, "Characterization of a zeolite-templated carbon by electrochemical quartz crystal microbalance and in situ Raman spectroscopy," *Carbon*, vol. 89, pp. 63–73, 2015.